Collective modes of the two-dimensional Wigner crystal in a strong magnetic field

R. Côté* and A. H. MacDonald
Department of Physics, Indiana University, Bloomington, Indiana 47405
(Received 25 February 1991; revised manuscript received 24 June 1991)

We present a calculation of the dispersion relation of the intra-Landau-level and inter-Landau-level collective modes of the two-dimensional Wigner crystal in a strong magnetic field. Our analysis is based on the time-dependent Hartree-Fock approximation (TDHFA) for the density-density response function and allows for an arbitrary large degree of anharmonicity. We derive the density-density response function from an equation-of-motion approach that uses identities valid in the strong-field limit. The TDHFA response function is shown to depend only on the ground-state density as calculated in the Hartree-Fock approximation. The intra-Landau-level collective excitation and the excitation near the cyclotron frequency are shown to correspond, respectively, to the low- and high-energy branches of the harmonic phonon spectrum. Additional collective-excitation branches occur near larger multiples of the cyclotron frequency. In contrast with the Hartree-Fock approximation, the TDHFA excitation spectrum does not contain transitions between the Landau-level subbands created by the self-consistent Hartree-Fock potential in the electron lattice.

I. INTRODUCTION

A gas of electrons will form a Wigner[1] crystal at sufficiently low density and temperature when the energy cost of localizing electrons around lattice sites is outweighed by the decrease in the potential energy due to the formation of the lattice. Wigner crystallization has been observed in two-dimensional sheets of electrons trapped on the surface of liquid helium[2] where the electron gas is almost classical ($\hbar^2/m^*a_0^2 \ll k_B T$, $e^2/\epsilon a_0$, where a_0 is the lattice spacing and ϵ is the dielectric constant). However, at least in the absence of a magnetic field, there has been no observation of such a phase in the quantum regime, which usually applies for electrons in doped bulk semiconductors or in two-dimensional electron-gas (2DEG) systems formed at semiconductor inversion layers. The crystallization physics is qualitatively changed when a magnetic field is applied, especially for a 2DEG. In a magnetic field, electrons execute circular cyclotron orbits for which the energy is quantized in units proportional to the magnetic-field strength. In the strong-magnetic-field limit, all electrons have the minimum quantized kinetic energy, i.e., all are in the lowest Landau level. The large quantized kinetic energy allows the electrons to be localized to a length comparable to their classical cyclotron orbit radius without any further cost in kinetic energy. (The minimum kinetic energy is $\hbar\omega_c/2$, where $\omega_c = eB/m^*c$ is the cyclotron frequency. The corresponding cyclotron orbit radius is the magnetic length $l = \sqrt{\hbar c/eB}$, which decreases with increasing magnetic field.) Once l becomes small compared to the typical distance between electrons, crystallization will occur.[3,4] In zero field the Wigner crystal can only exist below some critical density. For any density, however, crystallization will occur for a sufficiently strong magnetic field.

In this paper attention is restricted to the case where all electrons are in the lowest Landau level and $\hbar\omega_c \gg e^2/a_0$ so that Landau-level mixing due to electron-electron interactions can be neglected. In this limit, because of the Landau-level degeneracy, the Coulomb interaction is the only essential term in the Hamiltonian and direct perturbative treatments of the physics are not possible. Wigner-crystal states with broken translational symmetry are in competition with the incompressible fluid states[5] responsible for the fractional quantum Hall effect,[6] which are especially stable when the filling factor $\nu = 2\pi l^2 n = nhc/eB$ is a fraction with an odd denominator (n is the areal electron density). Observations of the Wigner crystal have been claimed[7] in this regime, however, and suggest that the crystal phase is stable for filling factor $\nu \leq \frac{1}{4}$, except for ν near $1/m$ for $m = 5$ and possibly[8] larger odd integers. These observations are consistent with theoretical estimates[9] of the filling factor at which the transition to the crystallization state is expected. Anomalies seen in sound propagation,[10] which are not yet fully understood, might indicates that the ground state is also crystalline for ν near $\frac{1}{2}$.

The dispersion relations of the normal modes of the classical two-dimensional Wigner crystal in a magnetic field were evaluated by Bonsall and Maradudin.[11] The corresponding quantum-mechanical calculation was done by Fukuyama.[12] In the strong-field limit they find that the two phonon branches of the crystal are separated into a low-frequency nearly transverse branch and a high-frequency nearly longitudinal branch which occurs near the cyclotron frequency and, in the long-wavelength limit, corresponds to a classical magnetoplasmon. The unusual $k^{3/2}$ dispersion of the transverse phonon mode can provide a clear signature of the crystalline state. These calculations assume the usual harmonic approximation which requires that the displacement of a particle

from its equilibrium position in the lattice is small. Because of the large zero-point motion of an electron in the Wigner crystal (which is of the order of $l=\sqrt{\nu}/2\pi a_0 \approx 0.28 a_0$ at $\nu=\frac{1}{2}$), the harmonic approximation is, *a priori,* well justified only for very small filling factors even at zero temperature. One may expect that anharmonic effects due to this large zero-point motion, as well as short-range correlations resulting from the proximity of the particles during their relative motion, could modify the dispersion relation of the collective modes.

In the 1960s a number of techniques[13] were developed in order to deal with the lattice dynamics of systems for which the harmonic approximation is invalidated by zero-point motion. (The most conspicuous example of these so-called quantum crystals was solid helium.) The successful approaches are equivalent to an effective harmonic approximation in which the force constant is averaged over the motion of the particles. In this paper we derive the collective modes of the Wigner crystal in the strong-field limit using a formulation in which each electron is allowed to move itinerantly through the crystal rather than having its motion referred to a particular lattice site. Expansions in displacements from lattice sites do not appear at all. The collective modes are associated with poles of the density-density response function which we derive in the time-dependent Hartree-Fock approximation (TDHFA). We first solve for the ground-state density $\langle n(\mathbf{G})\rangle$ ($\mathbf{G}$ is a reciprocal lattice vector) in the Hartree-Fock approximation HFA and then show that the density-density response function can be derived from a relatively simple equation of motion which depends on $\langle n(\mathbf{G})\rangle$ only. The broken translational symmetry of the crystalline ground state is thus easily introduced in the calculation. The derivation of this equation of motion is facilitated by identities valid in the strong-field limit. In this limit the TDHFA response function (and thus the dynamical properties of the crystal) depend on the ground state density only. Our approach becomes exact in the harmonic limit ($\nu\rightarrow 0$), but allows for arbitrarily large anharmonicity at larger filling factors and is able to account for itinerant behavior of the electrons without any difficulty. We find that, for filling factor $\nu\leq\frac{1}{2}$, the TDHFA phonons are only slightly different from those calculated by the usual harmonic approximation.[11,12] For filling factor $\frac{1}{3}<\nu\leq 0.45$, however, exchange effects become important and very much modify the dispersion relation until the crystal starts to soften at $\nu\approx 0.45$. The TDHFA magnetoplasmon branch is also close to the results obtained in the harmonic approximation, at least over the range of filling factors where the ground state is expected to be crystalline. However, we find that additional collective modes occur near multiples of the cyclotron frequency. These modes are absent in the harmonic approximation and are analogous to excitations which occur in the fluid state.[14]

Our approach is formally close to the random-phase-approximation (RPA) phonon theory for quantum crystals developed by Brenig[15] and Fredkin and Werthamer[16] and reviewed in Ref. 17. This approach is based on a mean-field picture of the lattice ground state in which each particle moves in a self-consistent potential which attracts the particles to the lattice sites. The particles are assumed to be bound to the lattice sites so that, in the harmonic limit, an Einstein oscillator exists at each site. The phonon excitations of the lattice are identified with poles in the response of the displacement of each particle from its lattice site to an external potential. Each responding particle sees local fields from its interaction with the responding particles on other sites, and this leads to an effective harmonic problem with force constants determined by an average over the particle motion. Our approach improves on this approximation in several ways which are important for the present problem. Most importantly the particles are not assumed to be bound to a particular lattice site, but allowed to be itinerant. For itinerant particles it is essential to account for statistics and we are able to self-consistently include exchange in both the ground state and in the local fields. Once the particles are allowed to move throughout the crystal, it is no longer possible to identify a discrete degree of freedom such as the displacement of a particular particle from a particular lattice site. For this reason we formulate our theory in terms of the density-density response function, which is directly related to experiment, rather than the displacement-displacement response function, which appears naturally in the RPA-phonon theory.

This paper is organized in the following way. In Sec. II we derive a general expression for the Hartree-Fock Hamiltonian of the 2DEG in a magnetic field. We use the strong-field limit of this expression in Sec. III to derive an expression for the ground-state density $\langle n(G)\rangle$ of the Wigner crystal using an equation-of-motion approach. We then derive, in Sec. IV, the strong-magnetic-field density-density response function in the TDHFA. We present and discuss our numerical results in Sec. V. Finally, we summarize our results and make some concluding remarks in Sec. VI. A brief account of this work has appeared previously.[18] We remark that another calculation of the dispersion relation of the collective modes of the two-dimensional Wigner crystal using a different formalism (the self-consistent phonon formalism with the inclusion of the cubic anharmonic correction) has been done very recently by Esfarjani and Chui.[19] Some of their results are different from those obtained with our approach.

II. HARTREE-FOCK HAMILTONIAN

In this section we derive the Hartree-Fock Hamiltonian of the two-dimensional Wigner crystal including an arbitrary number of Landau levels, following the approach of Ref. 20. This allows us to define our notation and to introduce the formalism that we will use in the next sections to obtain the equations of motion of the one- and two-particle (density-density response function) Green's functions, from which we extract respectively the ground-state density and collective modes.

Working in the Landau gauge, we write, for the Hamiltonian of the two-dimensional electron gas subjected to a transverse magnetic field $\mathbf{B}=-B_0\hat{\mathbf{z}}$

$$H=\sum_{n,X}\varepsilon_n c^{\dagger}_{n,X}c_{n,X}+\frac{1}{2S}\sum_{\mathbf{q}}\sum_{n_1,X_1,\ldots,n_4,X_4} V(\mathbf{q})\langle n_1,X_1|\exp(i\mathbf{q}\cdot\mathbf{r})|n_4,X_4\rangle \times\langle n_2,X_2|\exp(-i\mathbf{q}\cdot\mathbf{r})|n_3,X_3\rangle c^{\dagger}_{n_1,X_1}c^{\dagger}_{n_2,X_2}c_{n_3,X_3}c_{n_4,X_4}\ , \tag{1}$$

where

$$\langle\mathbf{r}|n,X\rangle=\frac{1}{\sqrt{L_y}}\exp(iXy/l^2)\phi_n(x-X),\quad n=0,1,2,\ldots \tag{2}$$

are the eigenstates of the kinetic energy operator, $\phi_n(x)$ is a one-dimensional harmonic-oscillator eigenstate with oscillatory frequency $\omega_c=eB_0/m^*c$, $l=(\hbar c/eB_0)^{1/2}$ is the Larmor radius, and, for a finite system, the allowed values of the quantum number X are separated by $2\pi l^2/L_y$. The energy eigenvalues of the Landau levels n are given by $\varepsilon_n=\hbar\omega_c(n+\frac{1}{2})$ and are independent of X. The degeneracy of each Landau level is given by $g=S/2\pi l^2$, where S is the area of the two-dimensional electron gas. Finally $V(\mathbf{q})=2\pi e^2/q$ is the two-dimensional Fourier transform of the Coulomb potential. Note that we have assumed that the electron spin will be completely aligned with the external magnetic field in the strong-field limit of interest and have dropped the spin degree of freedom.

The matrix elements $\langle n,X|\exp(i\mathbf{q}\cdot\mathbf{r})|n',X'\rangle$ in Eq. (1) are given by

$$\langle n',X'|\exp(i\mathbf{q}\cdot\mathbf{r})|n,X\rangle=\exp[i\tfrac{1}{2}q_x(X'+X)]F_{n',n}(\mathbf{q})\delta_{X',X+q_yl^2}\ , \tag{3}$$

where

$$F_{n',n}(\mathbf{q})=\left[\frac{n!}{n'!}\right]^{1/2}\left[\frac{(-q_y+iq_x)l}{\sqrt{2}}\right]^{n'-n}\exp\left[\frac{-q^2l^2}{4}\right]L_n^{n'-n}\left[\frac{q^2l^2}{2}\right] \tag{4}$$

for $n\le n'$, where $L_n^{\alpha}(x)$ is the generalized Laguerre polynomial. Note that $F_{n,n'}(\mathbf{q})=[F_{n',n}(-\mathbf{q})]^*$.

In the Landau eigenstates basis, the Fourier-transformed density operator $n(\mathbf{q})=\int d\mathbf{r}\exp(-i\mathbf{q}\cdot\mathbf{r})n(\mathbf{r})$ takes the form

$$n(\mathbf{q})=g\sum_{n,n'}\rho_{n,n'}(\mathbf{q})F_{n,n'}(-\mathbf{q})\ , \tag{5}$$

where we have introduced the operator

$$\rho_{n,n'}(\mathbf{q})=\frac{1}{g}\sum_{X}\exp(-iq_xX-\tfrac{1}{2}iq_xq_yl^2)c^{\dagger}_{n,X}c_{n',X+q_yl^2}\ , \tag{6}$$

which satisfies

$$\sum_n\rho_{n,n}(\mathbf{q}=0)=\frac{N}{g}\ , \tag{7}$$

where N is the number operator. $\nu=\langle N\rangle/g$ is the Landau-level filling factor of the electron gas. We shall work with the operator ρ instead of n in most of this paper. Equation (5) can be used to relate the equations derived below to equations for the density operator n.

Inverting Eq. (7), we get the relation

$$c^{\dagger}_{n,X}c_{n',X'}=\sum_{\mathbf{p}}\rho_{n,n'}(\mathbf{p})\exp[\tfrac{1}{2}ip_x(X+X')]\delta_{X,X'-p_yl^2}\ . \tag{8}$$

In the crystal phase the average density $\langle n(\mathbf{q})\rangle$ [and so $\langle\rho(\mathbf{q})\rangle$] is nonzero only at $\mathbf{q}=\mathbf{G}$. where $\mathbf{G}$ is a reciprocal-lattice vector of the two-dimensional lattice. It then follows from Eq. (8) that

$$\langle c^{\dagger}_{n,X}c_{n',X'}\rangle=\sum_{\mathbf{G}}\langle\rho_{n,n'}(\mathbf{G})\rangle\exp[\tfrac{1}{2}iG_x(X+X')]\delta_{X,X'-G_yl^2}\ . \tag{9}$$

Making the usual Hartree-Fock pairing of the second-quantized operators in the Hamiltonian of Eq. (1) and using Eq. (9), we get the Hartree-Fock approximation for H,

$$H_{\mathrm{HF}}=g\sum_n\varepsilon_n\rho_{n,n}(\mathbf{G}=0)+g\sum_{\mathbf{G}}\sum_{n,n'}U(n,n';\mathbf{G})\rho_{n,n'}(\mathbf{G})\ , \tag{10}$$

where we have defined an effective potential $U(n,n';\mathbf{G})$ by

$$U(n,n';\mathbf{G})=\sum_{n_1,n_2}\frac{e^2}{l}[H(n_1,n_2,n,n';\mathbf{G})-X(n_1,n',n,n_2;\mathbf{G})]\langle\rho_{n_1,n_2}(-\mathbf{G})\rangle\ , \tag{11}$$

with the Hartree (H) and Fock (F) terms defined by

$$H(n_1,n_2,n_3,n_4;\mathbf{G})=\frac{1}{2\pi e^2 l}V(\mathbf{G})F_{n_1,n_2}(\mathbf{G})F_{n_3,n_4}(-\mathbf{G}) , \tag{12a}$$

$$X(n_1,n_2,n_3,n_4;\mathbf{G})=\frac{l}{e^2 S}\sum_{\mathbf{q}} V(\mathbf{q})F_{n_1,n_2}(\mathbf{q})F_{n_3,n_4}(-\mathbf{q})\exp(-i\mathbf{q}\times\mathbf{G}l^2) . \tag{12b}$$

(We note that our definitions for these functions are slightly different from those of Ref. 20. Throughout this paper we use the two-dimensional cross product as a short form for $\mathbf{k}\times\mathbf{q}\equiv k_x q_y - k_y q_x$.)

III. GROUND-STATE DENSITY IN THE STRONG-FIELD LIMIT

We now derive the average density $\langle\rho(\mathbf{G})\rangle$ in the strong-field limit of the HFA using an equation-of-motion approach. As will be shown in Sec. IV $\langle\rho(\mathbf{G})\rangle$ is the only quantity needed to calculate the collective excitations of the Wigner crystal in the time-dependent Hartree-Fock approximation. In the strong-field limit $\hbar\omega_c \gg e^2/l$ ($\nu<1$), the HF Hamiltonian can be simplified by assuming that only the first Landau level ($n=0$) is partially occupied, i.e., that Landau-leveling mixing may be neglected. The Hilbert space may then be restricted to the lowest Landau level only. Magnetic fields where this approximation is well justified[20,21] are readily reached experimentally. Most of the results that we describe in this section have been obtained by early workers on the strong-magnetic-field Wigner crystal[22–25] using other approaches which prove to be far more cumbersome. We show, for completeness, how these results may be obtained using our equation-of-motion approach, establishing in this way some results required for the application of the equation-of-motion approach to the density-density response function.

Within the HFA the homogeneous electron gas becomes unstable with respect to the formation of a charge-density-wave (CDW) state below a temperature T_c, which is typically much higher than the melting temperature of the classical Wigner crystal.[22,23,25] It is usually assumed that strong short-range correlations exist below this temperature, although long-range order is not expected to survive the inclusion of correlations absent in the HFA, at least until much lower temperatures are reached. Many possible periodicities for the CDW are possible. At $T=0$ K, however, the configuration of lowest energy is assumed, for $\nu<\frac{1}{2}$, by a CDW with hexagonal symmetry and having one electron per unit cell.[26,27] (For ν very close to $\nu=\frac{1}{2}$, the square lattice is slightly lower in energy.) We refer to this particular CDW state as the triangular Wigner-crystal state since it approaches the classical Wigner crystal, where electrons are localized on the sites of a triangular lattice, for $\nu\ll 1$. (For a classical two-dimensional array of point charges, the configuration of lowest Coulomb energy is the triangular lattice.[11]) The density in the triangular Wigner-crystal phase is given by $n=1/\epsilon a_0^2$, where $\epsilon=\sqrt{3}/2$. Because of the electron-hole symmetry of the Hamiltonian, the properties of the system for $\frac{1}{2}<\nu<1$ may be obtained from that of the system with filling factor $1-\nu$ by replacing electrons by holes. Thus only the case $0<\nu<\frac{1}{2}$ needs to be considered.

The problem of finding the eigenstates and eigenenergies of electrons in the crystal phase of the HFA is complicated because these electrons feel both the external magnetic field and self-consistent periodic potential that they themselves create. It is known, however, from the study of noninteracting electrons in an external periodic potential[28,29] that, in this case, the Landau levels are split into subbands. Specifically, for the Wigner-crystal case, when the filling factor is rational, i.e., for $p/q=BS_0/\Phi_0=1/\nu$, where p and q have no factors in common and $S_0=n^{-1}$ is the unit-cell area of the crystal, the Landau level splits into p nonoverlapping subbands. For these rational filling factors, it is possible to block diagonalize the Hartree-Fock Hamiltonian into blocks of finite dimension d, where d is proportional to the number of subbands at the filling factor considered.[30] The diagonalization of these blocks is then performed numerically. The single-electron energies are given by $E_n(\mathbf{k})=\hbar\omega_c/2+\varepsilon_n(\mathbf{k})$, $n=1,2,\ldots,p$, where $\mathbf{k}$ is a vector restricted to the Brillouin zone of the crystal considered. The HFA single-electron spectra has been accurately evaluated by Yoshioka and Lee,[21] who find that the energy width of the occupied subband decreases sharply as the filling factor decreases toward zero. In the harmonic limit ($\nu\to 0$), the electrons are correspondingly increasingly localized around each lattice site and we expect the harmonic approximation to be accurate. The HFA charge density can be evaluated by summing over occupied states. (The effects of the Landau-level mixing as well as corrections to the HFA for the crystalline state are considered in Refs. 20, 21, and 26.)

If we are only interested in calculating the quantity $\langle\rho(\mathbf{G})\rangle$, a simpler numerical approach can be employed. To show this we begin by defining, using the finite-temperature Matsubara formalism,[31] the single-particle Green's function

$$G_{n,n'}(X,X',\tau)=-\langle Tc_{n,X}(\tau)c^{\dagger}_{n',X'}(0)\rangle \tag{13}$$

and its Fourier transform $G_{n,n'}(\mathbf{G},\tau)$ by

$$G_{n,n'}(\mathbf{G},\tau)=g^{-1}\sum_{X,X'} G_{n,n'}(X,X',\tau)\times\exp[-\tfrac{1}{2}iG_x(X+X')]\delta_{X',X-G_y l^2} , \tag{14}$$

so that $\langle\rho_{n,n'}(\mathbf{G})\rangle$ is given by

$$\langle \rho_{n,n'}(\mathbf{G}) \rangle = G_{n',n}(\mathbf{G}, \tau = 0^-) \ . \tag{15}$$

Using

$$\hbar \frac{\partial}{\partial \tau}(\cdots) = [H - \mu N, (\cdots)] \ , \tag{16}$$

where μ is the chemical potential of the electrons which we measure with respect to the kinetic energy of the first Landau level, we obtain

$$[i\omega_n - (n\omega_c - \mu/\hbar)] G_{n,n'}(\mathbf{G}, \omega_n) - \sum_{n'',\mathbf{G}'} \frac{1}{\hbar} U(n, n'' \mathbf{G}' - \mathbf{G}) \times \exp[\tfrac{1}{2} i \mathbf{G} \times \mathbf{G}' l^2] G_{n'',n'}(\mathbf{G}', \omega_n) = \delta_{n,n'} \delta_{\mathbf{G},0} \ , \tag{17}$$

where ω_n is a fermionic Matsubara frequency. We now invoke approximations which are justified in the strong-field limit. First, we may assume that only the lowest Landau level is partially occupied, which allows us to take $\langle \rho_{n,n'}(\mathbf{G}) \rangle \neq 0$ only if n and n' are both zero. Equation (7) then becomes

$$\langle \rho(\mathbf{G}=0) \rangle \equiv \langle \rho_{0,0}(\mathbf{G}=0) \rangle = \nu \ , \tag{18}$$

and the effective potential reduces to

$$U(n,n';\mathbf{G}) = \frac{e^2}{l} [H(0,0,n,n';\mathbf{G}) - X(0,n',n,0;\mathbf{G})] \langle \rho(\mathbf{G}) \rangle \ . \tag{19}$$

Second, if the Landau levels are well separated, the large Landau-level separations render the parts of the effective potential which mix Landau levels ineffective. We may thus take

$$U(n,n';\mathbf{G}) \simeq U(n,n;\mathbf{G}) \delta_{n,n'} \equiv W_n(\mathbf{G}) \langle \rho(\mathbf{G}) \rangle \ , \tag{20}$$

which defines the effective interaction $W_n(\mathbf{G})$. With these approximations defining our lowest Landau-level approximation (LLLA), the equation of motion for $G_{0,0}(\mathbf{G}, \omega_n)$ becomes

$$(i\omega_n + \mu/\hbar) G_{0,0}(\mathbf{G}, \omega_n) - \sum_{\mathbf{G}'} A(\mathbf{G}, \mathbf{G}') G_{0,0}(\mathbf{G}', \omega_n) = \delta_{\mathbf{G},0} \ , \tag{21}$$

where we have defined the Hermitian matrix

$$A(\mathbf{G}, \mathbf{G}') = \frac{1}{\hbar} W_0(\mathbf{G} - \mathbf{G}') \langle \rho(\mathbf{G} - \mathbf{G}') \rangle \times \exp[\tfrac{1}{2} i \mathbf{G} \times \mathbf{G}' l^2) \ . \tag{22}$$

The effective interaction $W_0(\mathbf{G})$ has the explicit form

$$W_0(\mathbf{G}) = \frac{e^2}{l} \left[\frac{1}{Gl} e^{-G^2 l^2/2} (1 - \delta_{\mathbf{G},0}) - \left[\frac{\pi}{2} \right]^{1/2} e^{-G^2 l^2/4} I_0(G^2 l^2/4) \right] \equiv \frac{e^2}{l} [H_0(G)(1 - \delta_{G,0}) - X_0(G)] \ , \tag{23}$$

where $I_0(x)$ is the modified Bessel function of the first the kind (the factor $1 - \delta_{\mathbf{G},0}$ is due to the neutralizing positive background). $W_0(\mathbf{G})$ is plotted in Fig. 1.

Using the eigenvalues and eigenvectors of $A(\mathbf{G}, \mathbf{G}')$ defined by

$$\sum_{\mathbf{G}'} A(\mathbf{G}, \mathbf{G}') V(\mathbf{G}', j) = V(\mathbf{G}, j) \omega_j \ , \tag{24}$$

and performing a Matsubara-frequency sum, we can express the ground-state density as

$$\langle \rho(\mathbf{G}) \rangle = \sum_j V(\mathbf{G}, j) [V(\mathbf{G}=0, j)]^* f(\hbar \omega_j - \mu) \ , \tag{25}$$

where $f(x) = [\exp(\beta x) - 1]^{-1}$ is the Fermi distribution function with $\beta = 1/k_B T$. At $T = 0$ K we can easily derive, using this last equation, the sum rule

$$\sum_{\mathbf{G}} \langle \rho(\mathbf{G}) \rangle^2 = \sum_j V(\mathbf{G}=0, j) [V(\mathbf{G}=0, j)]^* f(\hbar \omega_j - \mu)]^2 \rightarrow \sum_j V(\mathbf{G}=0, j) [V(\mathbf{G}=0, j)]^* \Theta(\mu - \hbar \omega_j) = \langle \rho(\mathbf{G}=0) \rangle = \nu \ . \tag{26}$$

This sum rule was derived previously, although in a more complicated way, in Ref. 21. Finally, the ground-state energy per particle is now simply given by

$$E_{\mathrm{HF}} = \frac{\hbar \omega_c}{2} + \frac{1}{2\nu} \sum_{\mathbf{G}} W_0(\mathbf{G}) \langle \rho(\mathbf{G}) \rangle^2 = \frac{\hbar \omega_c}{2} + \frac{1}{2\nu} \frac{e^2}{l} \sum_{\mathbf{G}} [H_0(G)(1 - \delta_{G,0}) - X_0(G)] \times \langle \rho(\mathbf{G}) \rangle^2 \ . \tag{27}$$

Since the effective interaction $W_0(\mathbf{G})$ is negative for $Gl \geq 1$, we see that the HFA will possess a number of CDW solutions.[26] Equations (18), (24), and (25) and at

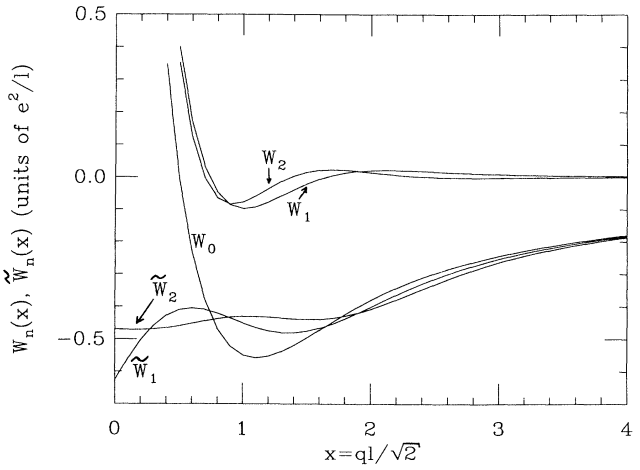

FIG. 1. Effective interactions $W_n(q)$ and $\tilde{W}_n(q)$ for $n = 0, 1, 2$ as defined in Eqs. (23), (51), and (52). [Note that $\tilde{W}_0(q) = W_0(q)$.]

$T=0$ K, the sum rule of Eq. (26) can be solved numerically to find a self-consistent solution for the density and chemical potential. To enforce a particular solution (we consider in this paper the case of a triangular Wigner crystal only), an external potential with the desired symmetry is added to the first iteration to the above set of equations. Of course, because the number of reciprocal-lattice vectors (and so the dimension of the matrix A) increases very rapidly with G, the approach presented here is useful only if the effective potential $U(0,0;\mathbf{G})$ decreases rapidly with G. We have found that for ν not too small (typically $\frac{1}{10}<\nu<\frac{1}{2}$), a rapidly convergent solution can be found by keeping a relatively small number of shells of reciprocal-lattice vectors (a shell contains all vectors of same modulus). In the above range for ν, the sum rule of Eq. (26) ($T=0$ K) was satisfied to more than six figures by keeping 16 shells of reciprocal-lattice vectors. Our results for the ground-state density and energy are in agreement with previous calculations using the block-diagonalization technique outlined at the beginning of this section.[21,26] It is, however, not possible to obtain the single-particle energies $E_n(\mathbf{k})$ with our approach. (We note that as the size of the matrix A is increased, the eigenvalues ω_j will fill in the bands of the single-particle energy spectrum, as expected.)

The ground-state density is well approximated,[23] in the small-filling-factor limit, by the Gaussian form

$$\langle\rho(G)\rangle_G=\nu\exp(-G^2l^2/4)\ , \tag{28}$$

which represents a Wigner crystal with a density pattern given by

$$\langle n(\mathbf{r})\rangle_G=\frac{1}{2\pi l^2}\sum_{\mathbf{R}_n}\exp[-(\mathbf{r}-\mathbf{R}_n)^2/2l^2]\ . \tag{29}$$

The wave function

$$|\phi(\mathbf{r})|^2=(1/2\pi l^2)\exp[(\mathbf{r}-\mathbf{R}_n)^2/2l^2]$$

is appropriate for an harmonic oscillator centered at $\mathbf{R}_n$ and having the zero-point energy $E_{zp}=\hbar\omega_c/2$. If we think of Eq. (29) as representing a set of N localized and independent oscillators, then the ground-state energy per particle of such a system would be given by

$$E_G=\frac{\hbar\omega_c}{2}+\frac{e^2}{l}\left[\frac{1}{2\nu}\sum_{\mathbf{G}\neq 0}H_0(G)\langle\rho(\mathbf{g})\rangle_G^2-\frac{\sqrt{\pi}}{4}\right] \tag{30}$$

where the first term in the large parentheses is simply the static Coulomb energy of a lattice with the density pattern of Eq. (29). For a lattice of point electrons ($l\ll a_0$), Eq. (30) simplifies to[11]

$$E_H=\frac{\hbar\omega_c}{2}-0.782\,133\sqrt{\nu}\left[\frac{e^2}{l}\right]\ . \tag{31}$$

The energy E_H represents a lower bound for the ground-state energy. The second term in the bracket of Eq. (30) is the self-interaction energy of an individual electron, which is implicitly included in the first term and must thus be removed. This self-interaction energy is also included in the first term in the bracket of Eq. (27) (the Hartree term), and in fact it can be seen from the numerical results that most of the Fock term in the HF ground-state energy serves to cancel this self-interaction energy, especially for $\nu\ll 1$. The net "exchange" contribution to the $E_{\rm HF}$ is thus quite small except for ν near $\frac{1}{2}$, where the overlap between wave functions of neighboring sites becomes significant (at $\nu=\frac{1}{2}$, $l/a_0\approx 0.28$).

In the LLLA the kinetic energy of the noninteracting electrons is frozen. The static correlations included in the HFA, however, give rise to an effective periodic potential at each lattice site in which the previously uncorrelated electrons now move. In the course of its large zero-point motion in this effective potential, the electron sees a restoring force that modifies its motion and changes its dynamic energy. In the ground state of the crystal, the electron has now a new zero-point energy and a modified wave function. The density pattern will thus also be modified. In the small-filling-factor limit, the HFA can be viewed as describing a set of uncorrelated oscillators oscillating with a renormalized frequency. As the filling factor increases, however, the electrons become more delocalized, the bandwidth of the occupied state increases, the electrons become more itinerant, and this picture is no longer applicable.

In Ref. 21 higher-order corrections to the HFA as well as Landau-level mixing are considered. These corrections modify the ground-state energy only slightly so that the HFA is indeed a very good approximation to the ground-state energy of the crystal state.[9] It is quite clear, however, from the large gap between occupied and unoccupied states in the single-particle energy spectrum that the HFA does not includes the correlations which give rise to the expected phononlike collective modes in the electron crystal. In the next section we describe how these collective excitations can be obtained starting from the HFA for the ground state. The above set of equations for $\langle\rho(G)\rangle$ can also be solved at finite temperature without further difficulty.[32]

IV. COLLECTIVE MODES IN THE TDHFA

Bonsall and Maradudin[11] have calculated the collective modes of the harmonic Wigner crystal for several different lattice types in two dimensions. For an electron lattice with a density pattern given by

$$n(\mathbf{r})=\sum_{\mathbf{R}_n}\sigma(\mathbf{r}-\mathbf{R}_n)\ , \tag{32}$$

the dynamical matrix is defined by

$$D_{\alpha,\beta}=\frac{1}{m}\sum_{\mathbf{R}}e^{-i\mathbf{k}\cdot\mathbf{R}}D_{\alpha,\beta}(\mathbf{R})\ , \tag{33}$$

where

$$D_{\alpha\beta}(\mathbf{R}_i-\mathbf{R}_j)=\frac{\delta^2}{\delta u_{i\alpha}\delta u_{j\beta}}\left[\frac{e^2}{2}\sum_{l\neq l'}\int d\mathbf{r}\int d\mathbf{r}'\frac{\sigma(\mathbf{r}-\mathbf{R}_l-\mathbf{u}_l)\sigma(\mathbf{r}'-\mathbf{R}'_{l'}-\mathbf{u}_{l'})}{|\mathbf{r}-\mathbf{r}'|}\right], \tag{34}$$

so that

$$D_{\alpha\beta}(\mathbf{k})=\frac{e^2}{m\epsilon a_0^2}\sum_{\mathbf{G}}[(\mathbf{k}+\mathbf{G})_\alpha(\mathbf{k}+\mathbf{G})_\beta V(\mathbf{k}+\mathbf{G})|\sigma(\mathbf{k}+\mathbf{G})|^2-\mathbf{G}_\alpha\mathbf{G}_\beta V(\mathbf{G})|\sigma(\mathbf{G})|^2]\ . \tag{35}$$

[As $\nu\to 0$, Eq. (35) must be cast into a more rapidly convergent form.[11]]

In the absence of a magnetic field, one finds, in the long-wavelength limit, a longitudinal normal mode with frequency $\omega_l\sim\sqrt{k}$ and a transverse normal mode with frequency $\omega_t\sim k$ corresponding to the plasmon and (transverse) phonon excitations of the crystal. The nonanalytic dispersion of the plasmon mode is due to the long-range nature of the Coulomb force and survives in the liquid phase, while the transverse phonon mode is specific to the crystalline phase. In the presence of a magnetic field, these two modes are coupled by the Lorentz force on the oscillating electrons. At long wavelength the coupling gives rise to a low-frequency $\omega_-\sim k^{1.5}$ magnetophonon mode and to a high-frequency magnetoplasmon mode with $\omega_+(k=0)=\omega_c$. In the strong-field limit the dispersion relation of these modes is given, using the identities $\omega_t^2+\omega_l^2=\mathrm{tr}(D)$ and $\omega_l^2\omega_t^2=\det(D)$,[11] by

$$\omega_-(\mathbf{k})=\frac{\omega_0^2}{\omega_c}\sqrt{\det[\tilde{D}(\mathbf{k})]} \tag{36a}$$

and

$$\omega_+(\mathbf{k})=\omega_c+\frac{\omega_0^2}{2\omega_c}\mathrm{tr}[\tilde{D}(\mathbf{k})]\ , \tag{36b}$$

where $\tilde{D}(\mathbf{k})=\omega_0^{-2}D(\mathbf{k})$ is a dimensionless quantity and $\omega_0^2=8e^2/ma_0^3$ sets the scale of the dynamical matrix. Since $\omega_0^2/\omega_c=(e^2/\hbar l)(\nu\sqrt{3}/\pi)^{1.5}$ is independent of the electron mass, we see that the magnetophonon mode corresponds, in the quantum picture, to an excitation of the Wigner crystal in which the quantized kinetic energy is not changed (i.e., to an intra-Landau-level excitation), while the magnetoplasmon corresponds to an excitation in which an electron is promoted to a higher Landau level (i.e., to an inter-Landau-level excitation).

In order to determine the spectrum of density fluctuations in the quantum crystal, we consider the density-density response function defined by

$$\chi_{n_1,n_2,n_3,n_4}(\mathbf{k}+\mathbf{G},\mathbf{k}+\mathbf{G}';\tau)=-g\langle T\tilde{\rho}_{n_1,n_2}(\mathbf{k}+\mathbf{G},\tau)\tilde{\rho}_{n_3,n_4}(-\mathbf{k}-\mathbf{G}',0)\rangle\ , \tag{37}$$

where $\tilde{\rho}_{n_1,n_2}=\rho_{n_1,n_2}-\langle\rho_{n_1,n_2}\rangle$ and $\mathbf{k}$ is a vector restricted to the first Brillouin zone. (Note that we again use the operator ρ instead of the true density operator n.) The strong-field limit of the classical results suggests that we can look for the corresponding quantum modes by calculating the poles of the functions $\chi_{0,0,0,0}$ for the magnetophonon and $\chi_{0,1,1,0}$ for the magnetoplasmon.

As we mentioned in the Introduction, the formalism that we use to derive the collective modes of the crystal is similar to the RPA-phonon technique reviewed in Ref. 17. However, as we saw in the preceding section, to obtain the CDW states it is necessary to include the exchange interaction in the mean-field Hamiltonian. To be consistent this exchange interaction must also be included in the derivation of response function. The resulting set of diagrams for this function includes ladder as well as bubble diagrams and is called the generalized random-phase approximation (GRPA) or time-dependent Hartree-Fock approximation. Ours are thus GRPA phonons instead of RPA phonons. Moreover, in the literature on quantum crystals, the particles are not allowed to move itinerantly and each particle is associated with a particular lattice site from which it is displaced. It is then natural to pursue the analogy with the harmonic approximation by defining the phonon frequency in terms of the positions of poles of a displacement-displacement response function. In this paper the displacement operator is not a useful quantity since its spectrum is unbounded. All collective modes are associated with poles of the density-density response function as is commonly the case in fluids. As a result, the quantities we calculate are much more directly related to experimental probes of the crystal.

It is easy to derive a general equation of motion for χ by making use of the commutation relation for the operators ρ_{n_1,n_2}, which is[33]

$$g[\rho_{n_1,n_2}(\mathbf{q}),\rho_{n_3,n_4}(\mathbf{q}')]=\rho_{n_1,n_4}(\mathbf{q}+\mathbf{q}')e^{i(1/2)\mathbf{q}\times\mathbf{q}'l^2}\delta_{n_2,n_3}-\rho_{n_3,n_2}(\mathbf{q}+\mathbf{q}')e^{-i(1/2)\mathbf{q}\times\mathbf{q}'l^2}\delta_{n_1,n_4}\ , \tag{38}$$

and of the HF Hamiltonian of Eq. (10). We obtain

$$
\begin{aligned}
&[i\Omega_n+(\varepsilon_{n_1}-\varepsilon_{n_2})/\hbar]\chi^0_{n_1,n_2,n_3,n_4}(\mathbf{k}+\mathbf{G},\mathbf{k}+\mathbf{G}';\Omega_n)\\
&\quad=\delta_{n_2,n_3}e^{-i(1/2)(\mathbf{k}+\mathbf{G})\times(\mathbf{k}+\mathbf{G}')l^2}\langle\rho_{n_1,n_4}(\mathbf{G}-\mathbf{G}')\rangle-\delta_{n_1,n_4}e^{i(1/2)(\mathbf{k}+\mathbf{G})\times(\mathbf{k}+\mathbf{G}')l^2}\langle\rho_{n_3,n_2}(\mathbf{G}-\mathbf{G}')\rangle\\
&\qquad-\frac{1}{\hbar}\sum_{\mathbf{G}''}\sum_n[U(n,n_1,\mathbf{G}''-\mathbf{G})e^{-i(1/2)(\mathbf{k}+\mathbf{G})\times(\mathbf{k}+\mathbf{G}'')l^2}]\chi^0_{n,n_2,n_3,n_4}(\mathbf{k}+\mathbf{G}'',\mathbf{k}+\mathbf{G}',\Omega_n)\\
&\qquad+\frac{1}{\hbar}\sum_{\mathbf{G}''}\sum_n[U(n_2,n,\mathbf{G}''-\mathbf{G})e^{i(1/2)(\mathbf{k}+\mathbf{G})\times(\mathbf{k}+\mathbf{G}'')l^2}]\chi^0_{n_1,n,n_3,n_4}(\mathbf{k}+\mathbf{G}'',\mathbf{k}+\mathbf{G}',\Omega_n)\ ,
\end{aligned}
\tag{39}
$$

where Ω_n is a boson frequency. Equation (39) corresponds to calculating χ in the HFA. (At this point since we have not yet made the LLLA.) We denote the HF result by χ^0. This function will have poles at single-particle transitions between the different subbands described in Sec. III. To get the collective modes we calculate χ in the time-dependent Hartree-Fock approximation. The TDHFA follows directly from a functional differentiation of the HFA (Ref. 34) equation of motion and is thus the natural approximation to take here since we have already calculated the ground state in the HFA. (The RPA comes from a functional differentiation of the Hartree approximation and corresponds to taking the irreducible part of χ, i.e., $\tilde{\chi}$, as given by single bubble diagram only instead of by the summation of ladder diagrams as in the TDHFA. The RPA phonons of Fredkin and Werthamer[16] are obtained in this way.) In the TDHFA the electrons respond to the changed Hartree and exchange local fields as well as to the external potential. Thus, in the harmonic limit, it is clear that, as an electron on one site is displaced from its lattice site, it will be subjected to a potential from the displacements of electrons on other sites so that the physics of the lattice dynamics will be captured.

The TDHFA is given by the set of equations

$$
\begin{aligned}
\chi_{n_1,n_2,n_3,n_4}(\mathbf{p}+\mathbf{G},\mathbf{p}+\mathbf{G}';\Omega_n)&=\tilde{\chi}_{n_1,n_2,n_3,n_4}(\mathbf{p}+\mathbf{G},\mathbf{p}+\mathbf{G}';\Omega_n)\\
&\quad+\frac{e^2}{\hbar l}\sum_{\mathbf{G}''}\tilde{\chi}_{n_1,n_2,n_5,n_6}(\mathbf{p}+\mathbf{G},\mathbf{p}+\mathbf{G}'';\Omega_n)H(n_5,n_6,n_7,n_8;\mathbf{p}+\mathbf{G}'')\\
&\quad\times\chi_{n_7,n_8,n_3,n_4}(\mathbf{p}+\mathbf{G}'',\mathbf{p}+\mathbf{G}';\Omega_n)
\end{aligned}
\tag{40}
$$

and

$$
\begin{aligned}
\tilde{\chi}_{n_1,n_2,n_3,n_4}(\mathbf{p}+\mathbf{G},\mathbf{p}+\mathbf{G}';\Omega_n)&=\chi^0_{n_1,n_2,n_3,n_4}(\mathbf{p}+\mathbf{G},\mathbf{p}+\mathbf{G}';\Omega_n)\\
&\quad-\frac{e^2}{\hbar l}\sum_{\mathbf{G}''}\chi^0_{n_1,n_2,n_5,n_6}(\mathbf{p}+\mathbf{G},\mathbf{p}+\mathbf{G}'';\Omega_n)X(n_7,n_6,n_5,n_8;\mathbf{p}+\mathbf{G}'')\\
&\quad\times\tilde{\chi}_{n_7,n_8,n_3,n_4}(\mathbf{p}+\mathbf{G}'',\mathbf{p}+\mathbf{G}';\Omega_n)
\end{aligned}
\tag{41}
$$

(where summation over repeated indices is implied). Note that the structure of these two equations with respect to momenta is very similar; i.e., the bubble and ladder diagrams sum in just the same way in the presence of a magnetic field. If we were to make the approximation of neglecting all Landau levels but $n=0$, we would write, for the full response function,

$$
\begin{aligned}
\chi(\mathbf{p}+\mathbf{G},\mathbf{p}+\mathbf{G}',\Omega_n)&=\chi^0(\mathbf{p}+\mathbf{G},\mathbf{p}+\mathbf{G}',\Omega_n)\\
&\quad+\frac{e^2}{\hbar l}\sum_{\mathbf{G}''}\chi^0(\mathbf{p}+\mathbf{G},\mathbf{p}+\mathbf{G}'',\Omega_n)[H_0(\mathbf{p}+\mathbf{G}'')-X_0(\mathbf{p}+\mathbf{G}'')]\chi(\mathbf{p}+\mathbf{G}'',\mathbf{p}+\mathbf{G}',\Omega_n)\ ,
\end{aligned}
\tag{42}
$$

which is just a RPA with an effective interaction given by H_0-X_0.

We shall now go to the strong-field limit and specialize to the case of $\nu<1$, making the LLLA described in Sec. III. It is easy to see, from Eq. (39), that the only nonzero HF response functions in this limit are given by $\chi^0_{0,n,n,0}(\mathbf{k}+\mathbf{G},\mathbf{k}+\mathbf{G}';\Omega_n)$ and $\chi^0_{n,0,0,n}(\mathbf{k}+\mathbf{G},\mathbf{k}+\mathbf{G}';\Omega_n)$. But because $\chi_{n_1,n_2,n_3,n_4}(\mathbf{k},\mathbf{k}';\Omega_n)=\chi_{n_3,n_4,n_1,n_2}(-\mathbf{k}',-\mathbf{k};-\Omega_n)$, we need only calculate $\chi^0_{0,n,n,0}(\mathbf{k}+\mathbf{G},\mathbf{k}+\mathbf{G}';\Omega_n)$.

Defining $\chi^0_{0,n,n,0}(\mathbf{k}+\mathbf{G},\mathbf{k}+\mathbf{G}';\Omega_n)\equiv\chi^{0(n)}_{\mathbf{G},\mathbf{G}'}(\mathbf{k};\Omega_n)$ and the matrices

$$
A^{(n)}_{\mathbf{G},\mathbf{G}'}(\mathbf{k})=\frac{1}{\hbar}W_n(\mathbf{G}-\mathbf{G}')\langle\rho(\mathbf{G}-\mathbf{G}')\rangle e^{-i(1/2)(\mathbf{k}+\mathbf{G})\times(\mathbf{k}+\mathbf{G}')l^2}\ ,
\tag{43}
$$

$$
B_{\mathbf{G},\mathbf{G}'}(\mathbf{k})=\langle\rho(\mathbf{G}-\mathbf{G}')\rangle e^{-i(1/2)(\mathbf{k}+\mathbf{G})\times(\mathbf{k}+\mathbf{G}')l^2}\ ,
\tag{44}
$$

$$
C_{\mathbf{G},\mathbf{G}'}(\mathbf{k})=\frac{2i}{\hbar}W_0(\mathbf{G}-\mathbf{G}')\sin[\tfrac{1}{2}(\mathbf{k}+\mathbf{G})\times(\mathbf{k}+\mathbf{G}')l^2]\langle\rho(\mathbf{G}-\mathbf{G}')\rangle\ ,
\tag{45}
$$

$$
D_{\mathbf{G},\mathbf{G}'}(\mathbf{k})=-2i\sin[\tfrac{1}{2}(\mathbf{k}+\mathbf{G})\times(\mathbf{k}+\mathbf{G}')l^2]\langle\rho(\mathbf{G}-\mathbf{G}')\rangle\ ,
\tag{46}
$$

these response functions obey the equations of motion (in an obvious matrix form)

$$\{(i\Omega_n - n\omega_c)I - [A^{(n)}(\mathbf{k})]^* + A^0(\mathbf{k})\}\chi^{0(n)}(\mathbf{k};\Omega_n) = B(\mathbf{k}) , \quad n \neq 0 \tag{47a}$$

$$[i\Omega_n I - C(\mathbf{k})]\chi^{0(0)}(\mathbf{k};\Omega_n) = D(\mathbf{k}), \quad n = 0 \tag{47b}$$

where I is the unit matrix. Note that in the strong-magnetic-field limit the HF response functions for different values of n are completely decoupled from one another. This decoupling persists in the full response function χ given by Eq. (40).

Defining the matrix

$$\tilde{W}^{(n)}_{\mathbf{G},\mathbf{G}'}(\mathbf{k}) = \delta_{\mathbf{G},\mathbf{G}'}\tilde{W}_n(\mathbf{k}+\mathbf{G}) , \tag{48}$$

where

$$\tilde{W}_n(\mathbf{k}) = \frac{e^2}{l}[H(n,0,0,n;\mathbf{k}) - X(0,0,n,n;\mathbf{k})] , \tag{49}$$

we have finally, for the response functions in the TDHFA,

$$\left[I(i\Omega_n - n\omega_c) - [A^{(n)}(\mathbf{k})]^* + A^0(\mathbf{k}) - \frac{1}{\hbar}B(\mathbf{k})\tilde{W}^{(n)}(\mathbf{k})\right]\chi^{(n)}(\mathbf{k};\Omega_n) = B(\mathbf{k}), \quad n \neq 0 \tag{50a}$$

$$\left[I(i\Omega_n) - C(\mathbf{k}) - \frac{1}{\hbar}D(\mathbf{k})\tilde{W}_0(\mathbf{k})\right]\chi^{(0)}(\mathbf{k};\Omega_n) = D(\mathbf{k}), \quad n = 0 . \tag{50b}$$

The interaction $W_n(k)$ that enters into the matrices A and C comes from the self-energy (Hartree and Fock terms) of an electron in level n due to the electrons in the lowest Landau level. The interaction $\tilde{W}_n(k)$ comes from the vertex corrections that take into account the direct and exchange interactions between the excited electron in level n and the hole left behind in level $n = 0$. These interactions have the explicit forms ($x = kl/\sqrt{2}$)

$$W_n(x) = \frac{e^2}{l}\left[\frac{1}{\sqrt{2}x}e^{-x^2}L_n(x^2)(1-\delta_{x,0}) - \frac{1}{n!}\left[\frac{\pi}{2}\right]^{1/2}e^{-x^2/2}Y_n(x)\right] \tag{51}$$

and

$$\tilde{W}_n(x) = \frac{e^2}{l}\left[\frac{1}{\sqrt{2}n!}e^{-x^2}x^{2n-1}(1-\delta_{x,0}) - \left[\frac{\pi}{2}\right]^{1/2}e^{-x^2/2}\sum_{m=0}^{n}(-1)^m\binom{n}{m}\frac{Y_m(x)}{m!}\right] \tag{52}$$

where $\binom{n}{m} = n!/(n-m)!m!$, $L_n(x)$ is the Laguerre polynomial, and we have defined the function

$$Y_n(x) = \frac{(-1)^n}{\pi 2^{2n-1}}\int_0^{\pi/2} d\theta\, e^{x^2\cos(2\theta)/2}H_{2n}(x\sin(\theta)) , \tag{53}$$

where $H_{2n}(x)$ is the Hermite polynomial. These potentials are plotted in Fig. 1. [Note that $\tilde{W}_0(x) = W_0(x)$. Also, $W_n(x=0)$ is finite since the Hartree contribution vanishes at $x = 0$ because of the uniform positive background.]

All response functions are thus obtained by an equation of the form $[(i\Omega_n - n\omega_c)I - M]\chi = N$, where M and N are matrices which depends only on the ground-state density $\langle\rho(G)\rangle$ evaluated in the HFA. (We remark that the response function $\chi_{n,0,0,n}(\mathbf{k}+\mathbf{G},\mathbf{k}+\mathbf{G}',i\Omega_n)$ obeys the equation of motion $[(i\Omega_n - n\omega_c)I - M]^*\chi_{n,0,0,n} = N^*$ so that $\chi_{n,0,0,n}(i\Omega_n) = [\chi_{0,n,n,0}(i\Omega_n)]^*$). The retarded response functions are obtained, as usual, by making the analytic continuation $i\Omega_n \to \omega + i\delta$.

It will be useful for the numerical analysis to write χ in the form $\chi = U[(\omega + i\delta - n\omega_c)I - P]^{-1}U^{-1}N$, where U and P, are respectively, the matrices of the eigenvectors $[U_{\mathbf{G},i}(\mathbf{k})]$ and eigenvalues $[\omega_i(\mathbf{k})]$ of M defined by $MU = UP$. Using Eq. (5) we have for the density-density response functions (defined with the "true" density operator n, not ρ the result

$$\Theta^{(n)}_{\mathbf{G},\mathbf{G}'}(\mathbf{k},\omega) = g\sum_i \frac{\sum_{\mathbf{G}''}F_{0n}(-\mathbf{k}-\mathbf{G})U_{\mathbf{G},i}(\mathbf{k})[U^{-1}(\mathbf{k})]_{i,\mathbf{G}''}N_{\mathbf{G}'',\mathbf{G}'}(\mathbf{k})F_{n0}(\mathbf{k}+\mathbf{G}')}{\omega + i\delta - [n\omega_c + \omega_i(\mathbf{k})]}$$

$$\equiv g\sum_i \frac{Z^{(n)}_{i,\mathbf{G},\mathbf{G}'}(\mathbf{k})}{\omega + i\delta - [n\omega_c + \omega_i(\mathbf{k})]} , \tag{54}$$

where $Z^{(n)}_{i,\mathbf{G},\mathbf{G}'}(\mathbf{k})$ is the weight of the pole at $\omega_i(\mathbf{k})$ in $\Theta^{(n)}_{\mathbf{G},\mathbf{G}'}(\mathbf{k},\omega)$. This is the form of our result used for the numerical calculations discussed in the next section.

Because of our LLLA, $\Theta^{(n)}_{\mathbf{G},\mathbf{G}'}(\mathbf{k},\omega)$, for $n \neq 0$, have poles at the positive frequencies given by $\omega = n\omega_c + \omega_i(\mathbf{k})$ only.

The corresponding poles at $\omega=-n\omega_c-\omega_i^*(\mathbf{k})$ are to be found in $\chi_{n,0,0,n}$, which, in terms of the "true" density operator and according to the remark made above, is simply given by $[\Theta^{(n)}_{\mathbf{G},\mathbf{G}'}(\mathbf{k},-\omega)]^*$. The full density-density retarded response function is thus, in our LLLA, given by

$$\Theta_{\mathbf{G},\mathbf{G}'}(\mathbf{k},\omega)=\Theta^{(0)}_{\mathbf{G},\mathbf{G}'}(\mathbf{k},\omega)+\sum_{n\neq 0}\{\Theta^{(n)}_{\mathbf{G},\mathbf{G}'}(\mathbf{k},\omega)+[\Theta^{(n)}_{\mathbf{G},\mathbf{G}'}(\mathbf{k},-\omega)]^*\}\ , \tag{55}$$

and $\Theta^{(0)}_{\mathbf{G},\mathbf{G}'}(\mathbf{k},\omega)$ has, of course, the same structure as the expression inside the curly brackets.

In concluding this section, we remark that in the liquid phase, where $\langle\rho(\mathbf{G})\rangle=\nu\delta_{\mathbf{G},0}$, Eqs. (50) can be trivially solved and give

$$\Theta^{(n)}_{\mathbf{G},\mathbf{G}'}(\mathbf{k},\omega)=\frac{N(1-\delta_{n,0})|F_{0n}(\mathbf{k}+\mathbf{G})|^2\delta_{\mathbf{G},\mathbf{G}'}}{\omega+i\delta-\omega_n(\mathbf{k}+\mathbf{G})}\ , \tag{56}$$

where the dispersion relation of the collective mode corresponding to the $0\rightarrow n$ excitation is given by

$$\omega_n(q)=n\omega_c+\frac{\nu}{\hbar}[W_n(0)-W_0(0)+\tilde{W}_n(q)] \tag{57}$$

for $n>0$. This dispersion relation is shifted by a self-energy correction $[W_n(0)-W_0(0)]=\frac{1}{2}\sqrt{\pi/2}$ $(n=1)$ or $\frac{5}{8}\sqrt{\pi/2}$ $(n=2)$ from the curve $\tilde{W}_n(x)$ represented in Fig. 1. In this limit our results for the excitation spectrum reduce to those obtained earlier.[35] The poles of the matrix $\Theta^{(n)}_{\mathbf{G},\mathbf{G}'}(\mathbf{k},\omega)$ are simply obtained by folding back the dispersion relation in the first Brillouin zone, i.e.,

$$\omega_i(\mathbf{k})=\omega_n(\mathbf{k}+\mathbf{G}_i)\ . \tag{58}$$

V. NUMERICAL RESULTS

Equations (47), (50), and (54) allow us to obtain the response functions $\Theta^{0(n)}$ and $\Theta^{(n)}$ and the dispersion relation of the collective modes by numerical matrix inversion or diagonalization of a single matrix. In identifying the excitation spectrum from the response function, it is sufficient to examine the imaginary part of the diagonal matrix element $\Theta^{(n)}_{\mathbf{G}=0,\mathbf{G}'=0}$. (All matrix elements share the same poles, but the poles are weighted differently in different matrix elements.) As in the calculation of the ground-state density, we have found that accurately convergent results are obtained by keeping 16 shells of reciprocal-lattice vectors (i.e., 127 vectors). The above formalism is completely general and thus is valid for finite temperatures. The temperature dependence appears entirely through the function $\langle\rho(G,T)\rangle$. In this paper we discuss only zero-temperature results.[32]

Figure 2(a) shows the imaginary part of the HF response function $\Theta^{0(0)}$ at filling factor $\nu=0.25$ and for two different values of the vector $\mathbf{k}$ in the irreducible Brillouin zone of the triangular lattice (see inset). The HF response function represents the response function of a system of uncorrelated electrons in the presence of a periodic potential as described in Sec. III and consequently the excitation spectrum consists of bands of particle-hole transition energies between the lower (filled) subbands and higher (unfilled) subbands. At $\nu=0.25$ the Landau level is split into four subbands, of which one is fully occupied so that transitions occur between the occupied (lowest) subband and three higher-energy subbands. For any truncation of the matrices in the reciprocal-lattice vector, the approximate response function has a finite number of simple poles; these poles merge into branch cuts as more reciprocal-lattice vectors are included. (As is clear from the logarithmic plots, the imaginary part is not exactly zero outside the single-particle-transition bands since we include only a finite number of reciprocal-lattice vectors.) We evaluate the response function with the frequency shifted from the real axis by an amount δ large enough to avoid resolving the individual poles. Only two peaks are visible in Fig. 2(a), because the highest two subbands are separated in energy by an amount comparable to the width of the occupied subband and partly because of the finite resolution with the value of δ chosen for the size of the matrix used. The imaginary part of the functions $\Theta^{0(1)}$ and $\Theta^{0(2)}$, corresponding to transitions to higher Landau levels, are shown in Figs. 2(b) and 2(c). In these figures three principal peaks are seen because the top two subbands of the higher Landau levels are also separated by a very small gap. (In calculating the response functions for $n>0$, we measure the excitation energy with respect to $n\hbar\omega_c$.) The excitations energies are shifted upward from $n\hbar\omega_c$ because the exchange self-energies are stronger for $n=0$ when the $n=0$ Landau level is occupied.[36] Although the position of the bands, for a given n, has almost no $\mathbf{k}$ dependence, there is a sharp increase in the intensity of the peaks as k increases in the irreducible Brillouin zone.

In Fig. 3(a) we show the imaginary part of the TDHFA response function $\Theta^{(0)}$ at filling factor $\nu=0.25$ and for the same two values of $\mathbf{k}$ in the irreducible Brillouin zone as in Fig. 2. The strong peaks with the large $\mathbf{k}$ dependence are the magnetophonons and have a typical energy of $0.05e^2/l$; this energy scale is comparable with the energy scale of the intra-Landau-level gap associated with the incompressible fractional-quantum-Hall states at nearby filling factors. Shown in the inset is the imaginary part of the function in the frequency range of the single-particle excitations [for point numbered 1 in Fig. 2(a)]. The TDHFA response function now shows absolutely no sign of these excitations. The correlations introduced by the TDHFA are sufficient to completely remove the independent-oscillator character of the electrons in the HFA. Figures 3(b) and 3(c) show the imaginary part of the response function for $n=1$ and 2. For $n=1$ the strong peaks in these figures correspond to the magnetoplasmon excitation of the harmonic lattice. For $n=2$ and similarly for $n>2$, the collective modes are the crystal analogs of the Berstein modes[14] which occur in the electron-fluid state. These are purely quantum excitations with no classical analog. Comparing Figs. 3(a), 3(b),

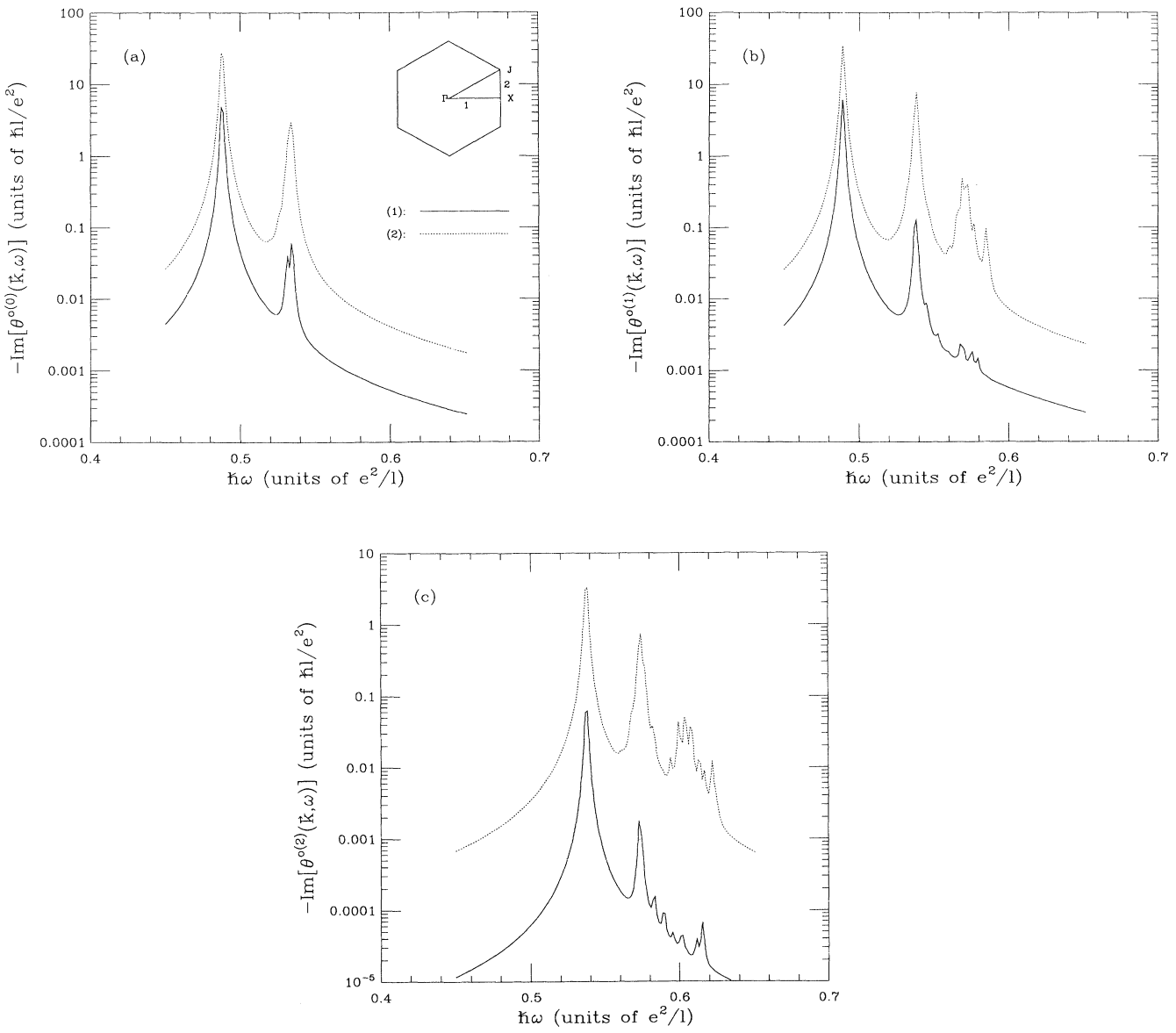

FIG. 2. Imaginary part of the HF response functions $\Theta^{0(n)}$, at filling factor $\nu=0.25$, evaluated at two different $\mathbf{k}$ values in the irreducible Brillouin zone of the triangular lattice as shown in the inset. The points $\Gamma=(0,0)$, $J=(1/\sqrt{3},\frac{1}{3})$, $X=(1/\sqrt{3},0)$, while $(1)=(\frac{1}{5},0)$ and $(2)=(1/\sqrt{3},\frac{1}{6})$. (All vectors are in $2\pi/a_0$ units.) The curves are for (a) $n=0$, (b) $n=1$, and (c) $n=2$. In (b) and (c), $\hbar\omega$ is measured with respect to $\hbar\omega_c$ and $2\hbar\omega_c$, respectively.

and 3(c), we see an indication that, as $\mathbf{k}$ goes to zero, the weights in the magnetophonon and Bernstein modes become much smaller than the weight in the magnetoplasmon mode. This result is in agreement with Kohn's theorem[37] which states that in the absence of an external potential and at long wavelength the response is dominated by an excitation in which the center-of-mass kinetic energy is increased by $\hbar\omega_c$. Note, however, that at larger wave vectors the weights of the different excitations become comparable. The dominance of the $n=1$ mode at long wavelength does not occur in the presence of an external potential, where Kohn's theorem does not apply, and is not seen in $\Theta^{0(n)}$, as we may see by comparing with Fig. 2. The translational invariance of the Hamiltonian is reflected when the consistent local-field corrections are added to the effective periodic potential of the HFA ground state.

All response functions show a set of other peaks at higher energies with decreasing strengths. These excitations have, as far as we can judge from our numerical results, a very small width, much smaller in fact than their energy and so appear to be well-defined excitations within

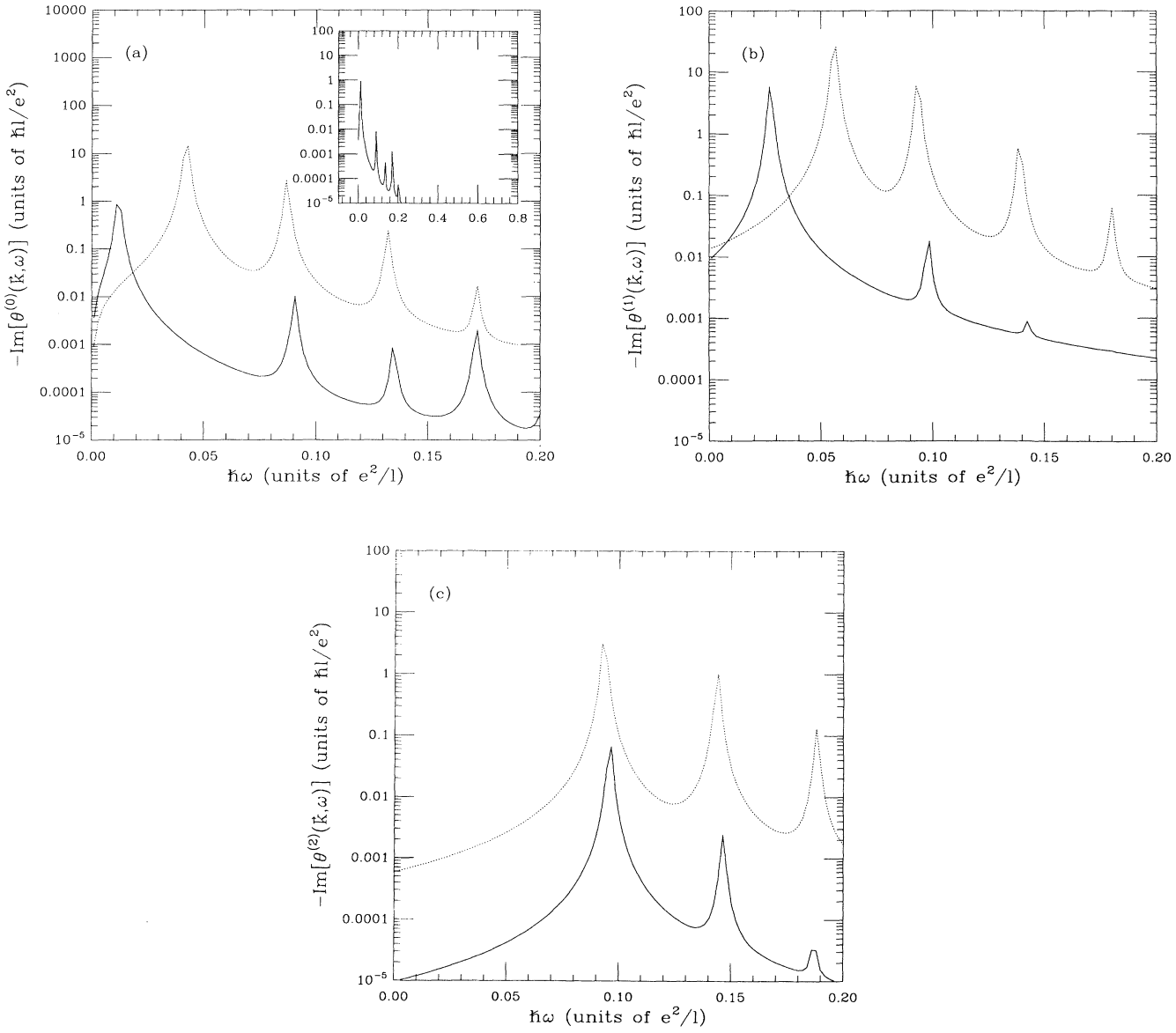

FIG. 3. Imaginary part of the TDHF response functions $\Theta^{(n)}$, at filling factor $\nu=0.25$ evaluated at the $\mathbf{k}$'s of Fig. 2 and for (a) $n=0$, (b) $n=1$, and (c) $n=2$. The solid curve is again the point labeled (1) in Fig. 2, while the dashed curve represents the point (2). The strong low-energy peaks in (a) and (b) correspond, respectively, to the magnetophonon and magnetoplasmon excitations. In the inset of (a) we show the results for point (1) over a wider range of frequencies. As can be seen, the single-particle transitions of Fig. 2 have completely disappeared in the TDHF response function. In (b) and (c), $\hbar\omega$ is measured with respect to $\hbar\omega_c$ and $2\hbar\omega_c$, respectively.

the TDHFA. As we increase the size of the matrix in the equation of motion, more and more of these excitations (at still higher energy) appear in the response function, while existing excitations suffer no shift in energy. These excitations are not numerical artifacts associated with the truncation of our infinite-dimensional matrices. Similar higher-energy excitations are also present in the RPA-phonon formalism,[17] where they can be identified as single-particle local-oscillator excitations. In that case they reflect the fact that the correlations in the RPA are not strong enough to completely remove the single-oscillator character of the Hartree electrons. Although we do not yet have a complete understanding of their origin we believe that these higher energy modes are truly physical and not an artifact of the TDHFA. Because the electrons are not just point particles, a full description of the density fluctuations must also contain information on the deformation of the electronic wave functions on length scales small compared to a lattice constant. In analogy with the liquid phase described at the end of the

last section [see Eq. (58)], the higher-energy modes probably are most usefully thought of as projections into the first Brillouin zone of a complete dispersion relation which extends to arbitrarily short wavelengths.

We identify the principal collective excitations with the pole of biggest weight in $\Theta^{(n)}$. As we mentioned previously, the magnetophonon is an intra-Landau-level excitation and appears as a pole of $\Theta^{(0)}$, while the magnetoplasmon is an inter-Landau-level excitation and appears as a pole of $\Theta^{(1)}$. In all cases the weight of the collective mode is much larger than that of the other (anharmonic) excitations so that the peak of the response may be identified as the excitation energy and the dispersion relation of the modes determined. We remark that the collective excitations are well defined in the TDHFA; i.e., the imaginary part of the pole is much smaller (at least 100 times smaller) than the real part, and so the excitation is long lived. In fact, we find that the imaginary part decreases as the size of the matrices in the equation of motion is increased. Because of technical limitations on

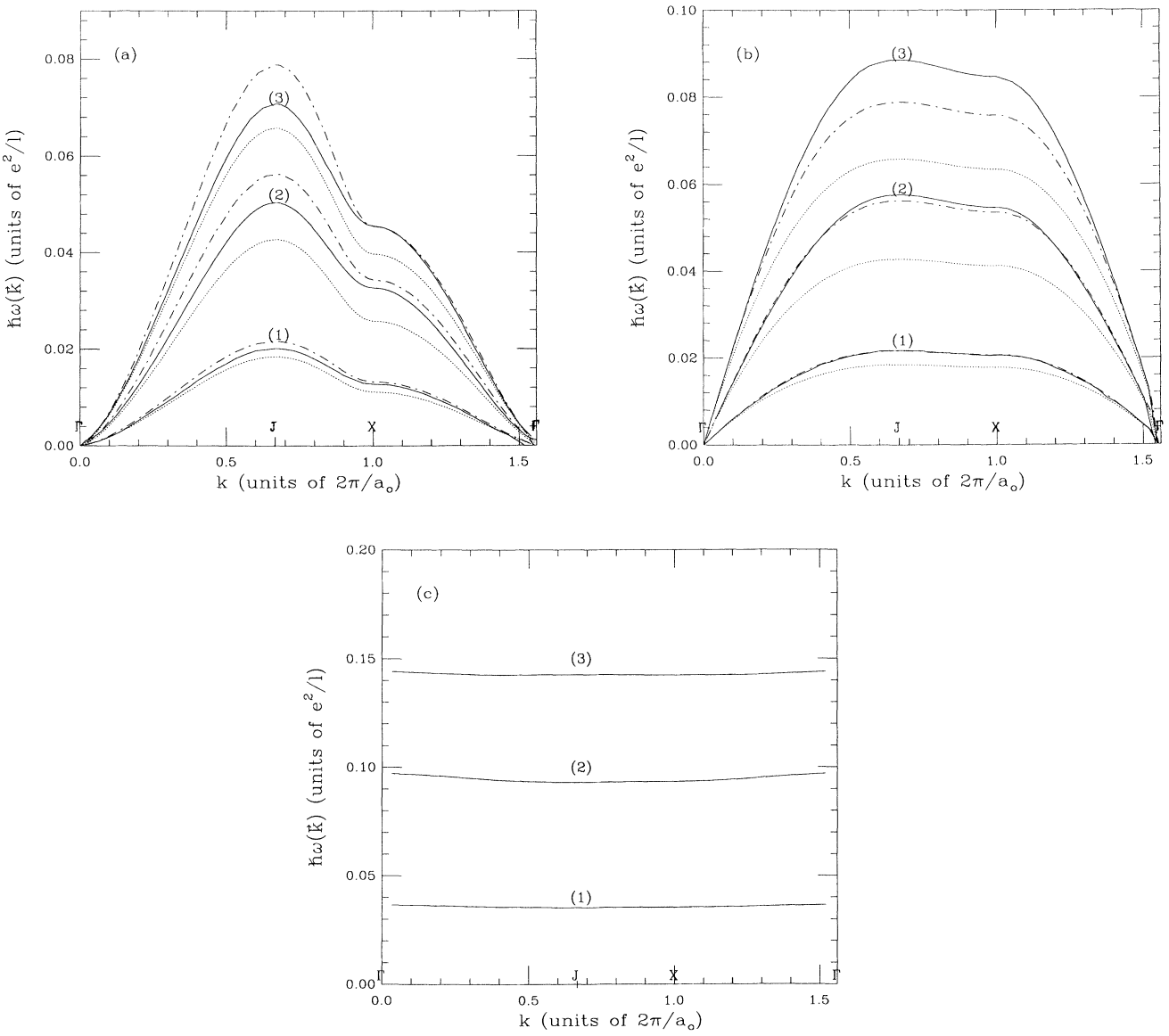

FIG. 4. Dispersion relations of the collective modes at filling factors (1) $\nu=\frac{1}{7}$, (2) $\nu=\frac{1}{4}$, and (3) $\nu=\frac{1}{3}$, for (a) magnetophonons, (b) magnetoplasmons, and (c) the $n=2$ excitation along the edges of the irreducible Brillouin zone of the triangular lattice shown in the inset of Fig. 2(a) (k here represents the total distance, in reciprocal space, along the path Γ-J-X-Γ from the origin Γ). The quantum dispersion relations are represented by the solid curves. In (a) and (b) the dotted curves (slightly below the solid curves) are the dispersion relation calculated for the harmonic lattice, while the dot-dashed curves (slightly above the solid curves) are the dispersion relation given by the "effective" dynamical matrix discussed in the text. In (b) and (c), $\hbar\omega$ is measured with respect to $\hbar\omega_c$ and $2\hbar\omega_c$, respectively.

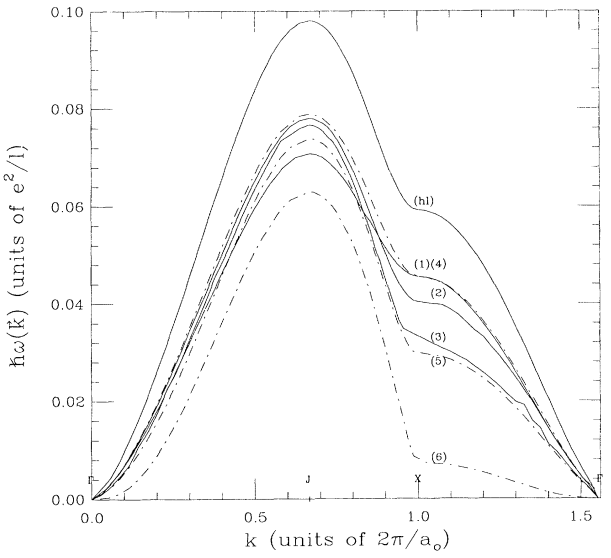

FIG. 5. Dispersion relations of the magnetophonons for filling factors $\nu=\frac{1}{3}$ for curves (1) and (4), $\nu=\frac{10}{23}$ for curves (2) and (5), and $\nu=\frac{7}{15}$ for curves (3) and (6) along the edges of the irreducible Brillouin zone (see Fig. 4). The quantum dispersion relations are represented by the solid curves (1)–(3). The dot-dashed curves numbered (4)–(6) represent the dispersion relations as calculated with the "effective" dynamical matrix discussed in the text. The curve labeled "hl" corresponds to the harmonic result at filling factor $\nu=\frac{10}{23}$.

the size of these matrices, we cannot set a lower value for the lifetime of these excitations within the TDHFA.

The dispersion relation of the collective modes for filling factors $\nu=\frac{1}{7}$, $\frac{1}{4}$, and $\frac{1}{3}$ are plotted in Figs. 4(a)–4(c). For the magnetophonon and magnetoplasmon modes, the quantum dispersion relation is compared with the dispersion relation calculated in the harmonic approximation. For $n=2$, where there is no corresponding harmonic excitation, the collective modes are much like the higher-energy anharmonic modes which occur for $n=0$ and 1 and have very weak dispersion. We see from Figs. 4(a) and 4(b) that the anharmonic corrections to the magnetophonon and magnetoplasmon dispersion relations are deceptively small for $\nu\leq\frac{1}{3}$ despite the large zero-point motion. The quantum effects (anharmonicity and exchange) begin to appear strongly for $\nu>\frac{1}{3}$ as shown in Fig. 5 for the magnetophonon dispersion relation (the magnetoplasmon dispersion relation has a similar behavior). In this figure the dispersion relation of the magnetophonons is plotted for $\nu=\frac{1}{3}$, $\frac{10}{23}$, $\frac{7}{15}$. For comparison we have also plotted the harmonic lattice result (the curve labeled "hl") at filling factor $\nu=\frac{10}{23}$. The energy of the phonon excitation seems to saturate at above $\nu=\frac{3}{7}$ as the filling factor is increased and then starts to decrease at $\nu\approx 0.45$. The numerical results become rather noisy at filling factors greater than 0.45 for the short-wavelength part of the spectrum (especially in the Γ-X direction of the irreducible Brillouin zone of the triangular lattice), while the long-wavelength part of the dispersion relation is well behaved. This indicates that the crystal becomes increasingly locally unstable at these filling factors. (A similar result was also found from a calculation of the shear modulus by Maki and Zotos[38] using a different approach.)

Because we do not introduce the displacement operator in our analysis, it is not easy to calculate an effective dynamical matrix from the observed dispersion relations. We can, however, get some feeling for what the effective dynamical matrix should be in the TDHFA by considering the following. The HF Hamiltonian giving rise to the ground-state energy of Eq. (27) can be interpreted as describing a system of electrons interacting through the effective interaction

$$V_{\rm eff}(\mathbf{q})=\frac{e^2}{l}(\nu\epsilon a_0^2)F_{00}^{-2}(q)[H_0(q)-X_0(q)]\ . \tag{59}$$

Assuming that the crystal can be described by the Gaussian density pattern of Eq. (29), we calculate the dynamical matrix of Eq. (35) with the Coulomb interaction V replaced by the effective interaction $V_{\rm eff}$. The dispersion relations given by this "effective" dynamical matrix is represented by the dot-dashed curve in Figs. 4 and 5. As we see, this effective dynamical matrix gives a better approximation to the quantum result than the harmonic approximation for $\nu\leq\frac{1}{3}$, while for $\nu>\frac{1}{3}$ it reproduces qualitatively the behavior of the quantum result. Clearly, the exchange interaction is very important for $\nu>\frac{1}{3}$ and is responsible for the softening of the crystal for $\nu>0.45$. Of course, a still better effective dynamical matrix would be obtained by allowing for the modification of the density pattern at larger filling factors.

VI. CONCLUSION

We have presented a new approach for the derivation of the collective modes of the Wigner crystal based on the calculation of the density-density correlation function. The interest of our approach is that it is not based on the assumption that the displacement of an electron from its lattice site is small so that it can account for an arbitrary degree of anharmonicity and can even allow for itinerant behavior of the electrons. Moreover, we calculated the density-density correlation function of in the TDHFA so that exchange interaction between the electrons is explicitly taken into account, both in the calculation of the ground state (through the HFA) and in that of the response function. In the high-magnetic-field limit, the response function was shown to obey a relatively simple equation of motion, thus simplifying greatly its numerical evaluation as well as that of its poles, i.e., of the collective modes of the crystal. We found that for filling factor $\nu\leq\frac{1}{3}$, the dispersion relation of the quantum magnetophonon and magnetoplasmon are not very much different from the dispersion relations calculated in the harmonic approximation. At larger filling factor, however, exchange effects become important and lead ultimately to a softening of the Wigner crystal at about $\nu=0.45$.

The formalism presented in this paper is also valid at finite temperature since the density-density correlation function depends on T through $\langle\rho(G,T)\rangle$ only. This quantity can be calculated, at finite temperature in the

HFA, using the approach developed in Sec. III in this paper. Since the HFA does not include the long-range correlations responsible for the collective modes, we do not expect the calculation of $\langle \rho(G,T) \rangle$ (and thus the calculation of the TDHFA response function, which is directly based on this quantity) to be directly relevant to the description of the Wigner-crystal melting. Moreover, since we are dealing here with a two-dimensional system, the melting is likely to be based on the Kosterlitz-Thouless mechanism.[9] The finite-temperature HFA results can be of interest, however, on a more local scale (i.e., for very small crystallites) where long-range fluctuations are irrelevant. The details of our results for the finite-temperature HFA and TDHFA will be presented elsewhere.[32]

ACKNOWLEDGMENTS

The authors acknowledge helpful discussions with S. M. Girvin, A. Griffin, G. D. Mahan, and P. M. Platzman. This work has been supported by the National Science Foundation under Grant No. DMR-8802383 and by the Natural Sciences and Engineering Research Council of Canada.

*Present address: Département de Physique, Université de Sherbrooke, Sherbrooke, Québec, Canada J1K 2R1.

[1]E. P. Wigner, Phys. Rev. **46**, 1002 (1934).
[2]C. C. Grimes and G. Adams, Phys. Rev. Lett. **42**, 795 (1979).
[3]F. P. Ulinich and N. A. Usov, Zh. Eksp. Teor. Fiz. **76**, 288 (1979) [Sov. Phys.—JETP **49**, 147 (1979)].
[4]M. Jonson and G. Srinivasan, Solid State Commun. **24**, 61 (1977).
[5]R. B. Laughlin, Phys. Rev. Lett. **50**, 1395 (1983).
[6]D. C. Tsui, H. L. Stormer, and A. C. Gossard, Phys. Rev. Lett. **48**, 1559 (1982).
[7]E. Y. Andrei, G. Deville, D. C. Glatti, F. I. B. Williams, E. Paris, and B. Etienne, Phys. Rev. Lett. **60**, 2765 (1988); V. J. Goldman, M. Shayegan, and D. C. Tsui, *ibid.* **61**, 881 (1988); R. L. Willett, H. L. Stormer, D. C. Tsui, L. N. Pfeiffer, K. W. West, and K. W. Baldwin, Phys. Rev. B **38**, 7881 (1988); D. C. Glattli, G. Deville, V. Duburcq, F. I. B. Williams, E. Paris, B. Etienne, and E. Andrei, Surf. Sci. **229**, 344 (1990); V. J. Goldman, M. Santos, M. Shayegan, and J. E. Cunningham, Phys. Rev. Lett. **65**, 2189 (1990); H. W. Jiang, R. L. Willett, H. L. Stormer, D. C. Tsui, L. N. Pfeiffer, and K. W. West, *ibid.* **65**, 633 (1990); M. A. Paalanen, R. L. Willett, P. B. Littlewood, R. R. Ruel, K. W. West, L. N. Pfeiffer, and D. J. Bishop (unpublished).
[8]H. Buhmann, W. Jose, K. von Klitzing, I. V. Kukushkin, G. Martinez, A. S. Plaut, K. Ploog, and V. B. Timofeev, Phys. Rev. Lett. **65**, 1056 (1990).
[9]Keivan Esfarjani and S. T. Chui, Phys. Rev. B **42**, 10 758 (1990); P. K. Lam and S. M. Girvin, *ibid.* **30**, 473 (1984); D. Levesque, J. J. Weis, and A. H. MacDonald, *ibid.* **30**, 1056 (1984).
[10]R. L. Willett, M. A. Paalanen, R. R. Ruel, K. W. West, L. N. Pfeiffer, and D. J. Bishop, Phys. Rev. Lett. **65**, 112 (1990).
[11]A complete derivation for different two-dimensional lattice types was done by L. Bonsall and A. A. Maradudin, Phys. Rev. B **15**, 1959 (1977). For earlier works, see also R. S. Crandall, Phys. Rev. A **8**, 2136 (1973); G. Meissner, H. Namaizawa, and M. Voss, Phys. Rev. B **13**, 1370 (1976); A. V. Chaplik, Zh. Eksp. Teor. Fiz. **62**, 746 (1972) [Sov. Phys.—JETP **35**, 395 (1972)].
[12]H. Fukuyama, Solid State Commun. **17**, 1323 (1975).
[13]For reviews of the extensive work done on this subject, see, for example, R. A. Guyer, in *Solid State Physics,* edited by F. Seitz, D. Turnbull, and H. Ehrenreich (Academic, New York, 1969), Vol. 23, p. 413, or C. M. Varma and N. R. Werthamer, in *The Physics of Liquid and Solid Helium,* edited by K. H. Bennemann and J. B. Ketterson (Wiley, New York, 1976).
[14]See, for example, E. Batke, D. Heitmann, and C. W. Tu, Phys. Rev. B **34**, 6951 (1986); A. V. Chaplik and D. Heitmann, J. Phys. C **18**, 3357 (1985).
[15]W. Brenig, Z. Phys. **171**, 60 (1963).
[16]D. R. Fredkin and N. R. Werthamer, Phys. Rev. **138**, A1527 (1965).
[17]For reviews, see N. R. Werthamer, Am. Phys. **37**, 763 (1969).
[18]R. Côté and A. H. MacDonald, Phys. Rev. Lett. **65**, 2662 (1990).
[19]K. Esfarjani and S. T. Chui (unpublished).
[20]A. H. MacDonald, Phys. Rev. B **30**, 4392 (1984).
[21]D. Yoshioka and P. A. Lee, Phys. Rev. B **27**, 4986 (1983).
[22]H. Fukuyama, P. M. Platzman, and P. W. Anderson, Phys. Rev. B **19**, 5211 (1979).
[23]D. Yoshioka and H. Fukuyama, J. Phys. Soc. Jpn. **47**, 394 (1979).
[24]Y. Kurmamoto, J. Phys. Soc. Jpn. **45**, 390 (1978).
[25]Rolf R. Gerhardts, Phys. Rev. B **24**, 1339 (1981).
[26]A. H. MacDonald and D. B. Murray, Phys. Rev. B **32**, 2291 (1985).
[27]F. Claro, Phys. Rev. B **35**, 7980 (1987).
[28]D. Hofstader, Phys. Rev. B **14**, 2239 (1976); F. Claro and G. Wannier *ibid.* **19**, 6068 (1979); A. H. MacDonald *ibid.* **28**, 6713 (1983); D. J. Thouless, M. Kohmoto, M. P. Nightingale, and M. den Nijs, Phys. Rev. Lett. **49**, 405 (1982).
[29]F. Claro and G. H. Wannier, Phys. Rev. B **19**, 6068 (1979).
[30]A. H. MacDonald, Phys. Rev. B **29**, 3057 (1984).
[31]See, for example, A. L. Fetter and J. D. Walecka, *Quantum Theory of Many-Particle Systems* (McGraw Hill, New York, 1971).
[32]R. Côté and A. H. MacDonald (unpublished).
[33]See, for example, *The Quantum Hall Effect: A Perspective,* edited by A. H. MacDonald (Kluwer, Boston, 1989).
[34]L. P. Kadanoff and G. Baym, *Quantum Statistical Mechanics* (Benjamin, New York, 1962).
[35]A. H. MacDonald, J. Phys. C **18**, 1003 (1985); C. Kallin and B. I. Halperin, Phys. Rev. B **30**, 5655 (1984); I. V. Lerner and Yu. E. Lozovik, Zh. Eksp. Teor. Fiz. **78**, 1167 (1978) [Sov. Phys.—JETP **51**, 588 (1980)].
[36]See, for example, A. H. MacDonald, H. C. A. Oji, and K. L. Liu, Phys. Rev. B **34**, 2681 (1986).
[37]W. Kohn, Phys. Rev. **123**, 1242 (1961).
[38]K. Maki and Z. Zotos, Phys. Rev. B **28**, 4349 (1983).